Beamforming Strategy Using Adaptive Beam Patterns and Power Control for Common Control Channel in Hierarchical Cell Structure Networks

Cheolwoo You, Young-Ho Jung, and Sunghyun Cho

Abstract: **Beamforming techniques have been successfully utilized for traffic channels in order to solve the interference problem. However, their use for control channels has not been sufficiently investigated. In this paper, a (semi-) centralized beamforming strategy that adaptively changes beam patterns and controls the total transmit power of cells is proposed for the performance enhancement of the common channel in hierarchical cell structure (HCS) networks. In addition, some examples of its practical implementation with low complexity are presented for two-tier HCS networks consisting of macro and pico cells. The performance of the proposed scheme has been evaluated through multi-cell system-level simulations under optimistic and pessimistic interference scenarios. The cumulative distribution function of user geometry or channel quality has been used as a performance metric since in the case of common control channel the number of outage users is more important than the sum rate. Simulation results confirm that the proposed scheme provides a significant gain compared to the random beamforming scheme as well as conventional systems that do not use the proposed algorithm. Finally, the proposed scheme can be applied simultaneously to several adjacent macro and pico cells even if it is designed primarily for the pico cell within macro cells.**

Index Terms: **Beamforming, beam pattern (BP), common control channel, hierarchical cell structure (HCS), power control.**

I. INTRODUCTION

Owing to the rapid growth in mobile communication over the past decade, various techniques have been developed to increase cellular network capacity. In particular, in some densely populated areas (referred to as "hot spots" [1]), small micro and pico cells are deployed beside macro cells to provide sufficient capacity. This scenario is often referred to as a hierarchical cell structure (HCS), in which different types of cells have overlapping coverage [2]. This type of cell structure allows the network to effectively cover the geographical area and also effectively serve an increasing population. The large cell (called a macro cell) is rearranged to include small cells called micro, pico, and femto cells.

Existing research on HCS systems has mainly focused on channel assignment in two-tier cellular radio systems [3], [4]. In general, orthogonal and cochannel methods can be used to share the radio spectrum [5], [6]. However, if we consider a mature macro cell network, the scarcity of radio resources and the ease of deployment, cochannel sharing would be more efficient and preferable for operators [7]; this fact is assumed in this paper. In such a situation, various and complicated interference scenarios are possible [8]. Therefore, controlling or mitigating interference between various types of cells in HCS networks is of paramount importance.

Many researchers have studied the problem of interference in HCS networks. This has resulted in proposals such as hybrid frequency assignments, the adjustment of the transmit (TX) powers of femtocell users, and the adaptive access operation of femtocells, to minimize cross-tier interference. Cancellation techniques have also been proposed but are often disregarded because of errors in the cancellation process. Techniques based on interference avoidance or randomization have been proposed as better alternatives. The use of sectorial antennas at the femtocell access point has also been suggested in [7] as a means of reducing interference; their use decreases the number of interferers. In order to avoid operator influence, decentralized strategies for interference management may be preferred by many researchers [7]. Nevertheless, if a (semi-) centralized strategy can be used with low complexity and cost, the possibility of performance improvement increases. In particular, it is more efficient for micro and pico cells.

As mentioned above, various research studies on HCS networks have been successfully carried out. However, most of the results are concerned with traffic channels that are generally intended for specific user(s). Since all mobile stations (MSs) should correctly receive common control channels, which are always transmitted by all base stations (BSs) and thus fully interfered, it is also very important to mitigate interference and reduce the outage probability of the channels. Nevertheless, research results on common control channels, especially those concerned with the successful use of beamforming for traffic channels, are scarce.

In this paper, on the basis of the above discussion, we propose a (semi-) centralized beamforming strategy involving the use of adaptive beam patterns (BPs), in combination with power control for performance enhancement of the common channel in HCS networks. Our main focus is on small cells rather than macro cells. Note that in this paper, we regard the frame control header (FCH) channel and the down-link manufacturing au-

Manuscript received November 29, 2010.

This research was supported by Basic Science Research Program through the National Research Foundation of Korea (NRF) funded by the Ministry of Education, Science and Technology (2011-0004634).

Cheolwoo You is with the Department of Information and Communication Engineering, Myongji University, Yongin 449-728, Korea, e-mail: cwyou@mju.ac.kr.

Young-Ho Jung is with the Department of Information and Telecommunication Engineering, Korea Aerospace University, Goyang 412-791, Korea, e-mail: yhjung@kau.ac.kr.

Sunghyun Cho is with the Department of Computer Science and Research Institute of Natural Science, Gyeongsang National University, Jinju 660-701, Korea, e-mail: dr.shcho@gnu.ac.kr.

tomation protocol (DL-MAP) used in IEEE 802.16e [9] since their performance on the cell edge are not good enough owing to interference from the adjacent cells/sectors and a low processing gain.

The remainder of this letter is organized as follows. In Section II, we describe the HCS network considered in this study and its related parameters. We also explain preliminary simulation results and the development strategy used. In Section III, we propose a beamforming strategy involving the use of BPs and power control and present a design example of the proposed algorithm. Section IV provides simulation results and comparisons obtained via system-level simulations. This is followed by our concluding remarks in Section V.

II. SYSTEM MODEL

A. Basic Assumptions and Key Parameters

An interesting HCS network consists of large and small cells. For simplifying the explanation and illustration, we assume, without loss of generality, that the large and small cells are macro and pico cells, respectively. In the HCS network, we assume that the macro cells are primary cells covering the entire network, with each macro BS having three sectors. In contrast, the pico cell is assumed to have only one sector and to use the same frequency as the macro cells. The macro cells are uniformly distributed, but the pico cells are randomly located within the macro cells since hotspot locations are likely to vary from one cell site to another and to be opportunistic rather than planned. Users in macro cells and pico cells are uniformly distributed inside the cell sites. We also assume that the pico cell is open to all user equipment (UE) and has a lower power, different antenna pattern, and different antenna height compared to the macro cell [10]–[12]. The TX power of the pico cell is approximately 1 W or less. The handover between the macro and pico cells follows the normal procedure that chooses the best sector with a hysteresis margin. Cells are probably connected to each other via the X2 interface [13].

The HCS network is assumed to include a central BS (CBS) that has a high-speed interface to communicate with other adjacent cells such as a central or super enhanced node B (eNB), and it can thus coordinately control adjacent macro and pico cells. Since the main role of the CBS considered in this study is the exchange of control information, the cost of implementation is low. In addition, one of the existing cells can take on the role of the CBS.

In order to investigate various scenarios for future mobile communication systems, many researchers have proposed propagation models. For example, the indoor small office has been studied in [14] and [15], where indoor hotspots have also been modeled. The outdoor-to-indoor scenario is the combination of an outdoor scenario and an indoor scenario, such as an urban micro cell and indoor small office. In the Winner II project [16], the various path loss scenarios were defined. Among these, B5a seems to be suitable for the line-of-sight (LOS) propagation between eNB and a fixed relay node (RN) and B5f seems suitable for non-LOS (NLOS) propagation between eNB and a fixed RN since B5a is for LOS from a rooftop to another rooftop and B5f is for LOS/NLOS from a rooftop to a location below/above another rooftop. The innovative micro technology evaluation (IMT-EVAL) path loss model [16] includes indoor hotspot, urban micro cell, urban macro cell, and rural macro cell scenarios.

Baseline path loss model applicable for the test scenarios in urban and suburban areas outside a high rise core where the

Table 1. Parameters for system-level simulation.

Parameter	Macro cell	Pico cell
Cell structure	Hexagonal grid, 3-tier, 19 cells, 3 sectors/site	1 sector/site
Number of MS per sector	20 active users	100–300 active users
BS max TX power (10 MHz carrier)	46 dBm	20–30 dBm
Cell radius (ISD/$\sqrt{3}$)	$1500/\sqrt{3}$ m	50–400 m
Path loss (dB)	$130.19+37.6\log_{10} R$	$150.94+40\log_{10} R$
- BS height	15 m+ average rooftop	About average rooftop
- MS height	1.5 m	1.5m
Shadow standard deviation	8 dB	4–8 dB (average 6 dB)
Min distance between UE and cell	>= 35 m	>= 7 m
BS antenna gain	17 dBi (boresight)	6 dBi with omni-antenna
Plus cable loss	− 2 dB (cable loss)	Without cable losses
Antenna pattern (BS)	70° sectored beam	Omni-direction

Parameter	Common in macro and pico cells
FFT size	1024
Duplexing scheme	TDD
Frame length	5 ms
Antenna pattern (MS)	Omni directional
Channel model	Rayleigh: 3 [Kmph]-30%, 10 [Kmph]-30% Rayleigh: 30 [Kmph]-20%, 120 [Kmph]-10% Rician: 10%
Center frequency	2.5 GHz
Bandwidth	10 MHz
Effective SINR	30 dB
Shadowing correlation	0.5 / 1.0 (between cells / sectors)
Correlation distance of shadowing	50 m
Penetration loss	10 dB
Thermal noise density	174 dBm/Hz
Noise figure	7 dB (UE), 5 dB (NB)
Uniform linear antenna array	BS antenna spacing: 4λ, MS antenna spacing: λ/2
CQI feedback	Ideal
Frequency reuse	Each sector with frequency reuse of 1

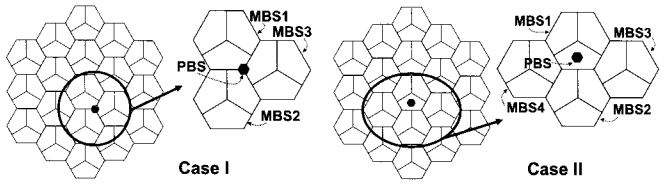

Fig. 1. Two contrasting cases for studying interference effects of the HCS network consisting of 19 macro cells (MBSs) and one pico cell (PBS).

buildings are of nearly uniform height is given by

$$PL\ (\text{dB}) = 40(1 - 4 \times 10^{-3} h_{\text{BS}}) \log_{10} R - 18 \log_{10} h_{\text{BS}} + 21 \log_{10} f + 80 \quad (1)$$

where R (Km) is the distance from the transmitter to the receiver, f (MHz) is the carrier frequency, and h_{BS} (m) is the BS antenna height above the rooftop [14], [17]. Applying a frequency correction factor of $21 \log_{10}(2.5/2)$ for operation at 2.5 GHz, (1) can be rewritten as

$$PL\ (\text{dB}) = 130.19 + 37.6 \log_{10} R. \quad (2)$$

The categorization of new nodes such as pico cells, home eNBs (femto cells), and relays is given in [10]–[12] for heterogeneous lay-outs. Since the new node antenna heights are much lower than those of the macro cells, new propagation models should be used. It is a good idea to use the international telecommunication union radiocommunication sector (ITU-R) outdoor-to-indoor model with the base station antenna height close to the rooftop level for the links between the new nodes and macro UE [11]:

$$PL\ (\text{dB}) = 49 + 40 \log_{10} R + 30 \log_{10} f. \quad (3)$$

For the carrier frequency of 2.5 GHz, (3) can be expressed as

$$PL\ (\text{dB}) = 150.94 + 40 \log_{10} R. \quad (4)$$

Table 1 shows key parameters, including the propagation models for the macro and pico cells; the parameters are selected on the basis of the above consideration. Note that (2) and (4) are used as the path loss models for macro and pico cells, respectively. We also note that in this paper, geometry represents the effects of long-term fading, path loss, interference, and all types of gains on the received signal-to-interference plus noise ratio (SINR). The channel quality indicator (CQI) additionally includes the effect of short-term fading in comparison with geometry.

B. Preliminary Simulation Results and Development Strategy

In order to study the interference effects of the HCS system, two contrasting cases, depicted in Fig. 1, are considered. Cases I and II are optimistic and pessimistic interference scenarios, respectively, from the viewpoint of the first macro BS (i.e., MBS1). Preliminary simulations for the two cases were performed using the parameters given in Table 1. From the simulation results, we drew several important points on the HCS network.

- The geometry of the macrocell (GMC) is almost unaffected by the location and TX power of the pico cell. However, it is dangerous to increase the TX power of pico cells above an appropriate level. In addition, changing of GMC can have a bad effect on the whole cell panning in a macro cellular network.
- The geometry of the pico cell (GPC) varies with the TX power of the pico cell. In addition, we can freely adjust the TX power of the pico cell within an appropriate level. Thus, the TX power of the pico cell is an important factor in the control of the pico cell performance.
- The user density of pico cells is usually higher than that of macro cells. The operator can preferentially assign high-data-rate users to a micro cell/pico cell since its capacity is inherently larger than that of the macro cell [3], [4]. Thus, in the boundary region between the pico and macro cells, if we want to improve the signal quality of one of the two cells, we had better choose the pico cell and develop an algorithm for the users belonging to the pico cell. That is, it is necessary to develop an algorithm for the performance improvement of the pico cell boundary users.
- Beamforming may be a good candidate and can be combined with the TX power control of the pico cell. That is, when the TX power of the pico cell is increased, harmful impacts on the macro cells can be minimized through beamforming.

III. BEAMFORMING STRATEGY USING BEAM PATTERNS AND POWER CONTROL

A. Proposed Scheme

Let us consider the downlink of a multi-cell wireless HCS system in which a BS with N TX antennas communicates simultaneously with M users who are dispersed geographically in one cell, at any given time slot t. For notational convenience, we assume that each user (or MS) has one receive antenna. In this case, we can model the channel matrix between the transmitter and the receivers with a complex $M \times N$ matrix $\mathbf{H}_t$, whose j, ith entry $h_{j,i}$ is the channel from TX antenna $i = 1, 2, \cdots, N$ to receiver $j = 1, 2, \cdots, M$ at time t. On the basis of the foregoing discussion, we also assume that one stream such as MAP is assigned to every user. Note that if some users have multiple receive (RX) antennas, the channel matrix can be easily extended and we can assume that they use the maximal-ratio combining (MRC) of received signals. In the following explanation, we have omitted the subscript t in all the notations where doing so does not cause ambiguity.

When the vector channel between the BS and the kth user is defined as $\mathbf{h}_k = [h_{k,1}\ \ h_{k,2}\ \ \cdots\ \ h_{k,N}]^T$, the channel matrix is given as

$$\mathbf{H} = [\mathbf{h}_1\ \ \mathbf{h}_2\ \ \cdots\ \ \mathbf{h}_M]^T. \quad (5)$$

where $(\cdot)^T$ denotes the transpose of the matrix. In general, we make no assumptions regarding the matrix H.

To change and control the BP, the proposed algorithm uses the beamforming (or precoding) matrix

$$\mathbf{F} = [\mathbf{f}_1\ \ \mathbf{f}_2\ \ \cdots\ \ \mathbf{f}_L] \quad (6)$$

where $\mathbf{f}_k$=$[f_{1,k}\ f_{2,k} \cdots f_{N,k}]^T$ with the constraint $|\mathbf{f}_k|^2 = 1$ and L is a positive integer. The proposed algorithm also uses an

$L \times 1$ power weight vector, $\mathbf{W}$, which is needed for the control of the total TX power (TTP) per sector/antenna within an upper limit (i.e., max TX power (MTP)) and is defined as

$$\mathbf{W} = [w_1 \;\; w_2 \;\; \cdots \;\; w_L]^T. \tag{7}$$

The elements of $\mathbf{W}$ are nonnegative real numbers. If the control channel (MAP) information bits consist of s, the $N \times 1$ TX vector $\mathbf{x}$ is defined as

$$\begin{aligned}\mathbf{x} &= \mathbf{FWs} \\ &= \left[\sum_{i=1}^{L} sf_{1,i}w_i \;\; \sum_{i=1}^{L} sf_{2,i}w_i \;\; \cdots \;\; \sum_{i=1}^{L} sf_{N,i}w_i\right]^T. \end{aligned} \tag{8}$$

Then, we can write the $M \times 1$ received vector as

$$\begin{aligned}\mathbf{y} &= [y_1 \;\; y_2 \;\; \cdots \;\; y_M]^T \\ &= \mathbf{Hx} + \mathbf{n} \end{aligned} \tag{9}$$

where y_k is the received signal at the receiver of the kth user that can be expressed as

$$y_k = s\sum_{j=1}^{N}\sum_{i=1}^{L} h_{k,j}f_{j,i}w_i + n_k, \tag{10}$$

and $\mathbf{n}$ is a vector of independent identically distributed zero-mean complex Gaussian noise entries with variance σ^2, whose kth element is the noise at the receiver of the kth user.

On the other hand, the codebook for the proposed algorithm can be defined as

$$\mathbf{C} = \{\mathbf{C}_1 \;\; \mathbf{C}_2 \;\; \cdots \;\; \mathbf{C}_R\} \tag{11}$$

where R is the size of the codebook. The rth element of (11) is an $N \times L$ matrix and a good choice for them is $\mathbf{C}_r^*\mathbf{C}_r = \mathbf{I}$. If it is assumed that the sub-codebook for the ith macro or pico cell is

$$\mathbf{Q}^i = \left\{\mathbf{Q}_1^i \;\; \mathbf{Q}_2^i \;\; \cdots \;\; \mathbf{Q}_{G(i)}^i\right\} \subset \mathbf{C} \tag{12}$$

where $G(i)$ is the size of the sub-codebook for the ith cell, the BP matrix selected for the ith macro or pico cell is given by

$$\mathbf{F}^i \triangleq \mathbf{F} \subset \mathbf{Q}^i. \tag{13}$$

For convenience in implementation, we can assume $L = 1$. In this case, we have

$$\mathbf{W} = w_1 \triangleq w, \tag{14}$$

$$\mathbf{F} = f_1 \triangleq \mathbf{f} = [f_1 f_2 \cdots \;\; f_N]^T \subset \mathbf{Q^i}, \tag{15}$$

$$y_k = sw(\mathbf{h}_k\mathbf{f}) + \mathbf{n}_k. \tag{16}$$

Assuming that the beamformer consists of a sector beamformer and a beamforming vector, the attenuation factor can be written as

$$\begin{aligned}\mathbf{A} &= \mathbf{e}_t(\Omega)^T\mathbf{f} \\ &= \frac{1}{\sqrt{N}}\sum_{k=1}^{N} e^{-j2\pi(k-1)\Delta_t\Omega}f_k, \end{aligned} \tag{17}$$

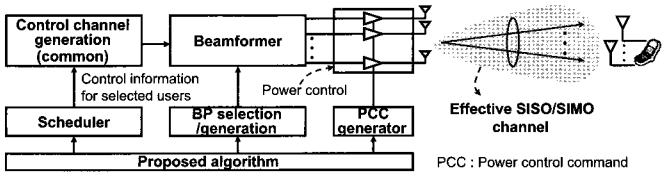

Fig. 2. One example of transmission system for the proposed algorithm.

where $\Omega = \cos\phi$, ϕ is the angle of departure of the LOS onto the antenna array, Δ_t is the normalized TX antenna separation, normalized to the unit of the carrier wavelength, and $\mathbf{e}_t(\Omega)$ is the unit spatial signature defined as

$$\begin{aligned}\mathbf{e}_t(\Omega) = &\frac{1}{\sqrt{N}} \\ &\cdot \left[1 \;\; e^{-j2\pi\Delta_t\Omega} \;\; e^{-j2\pi 2\Delta_t\Omega} \;\; \cdots \;\; e^{-j2\pi(N-1)\Delta_t\Omega}\right]^T. \end{aligned} \tag{18}$$

Then, for given ϕ and Δ_t, a signal in any other direction will be attenuated by a factor of $|\mathbf{A}|$.

In this paper, we assume that the proposed algorithm uses changes in the BP, control of TTP, modification of scheduling algorithm, or a combination of these factors. In this case, Fig. 2 shows one possible example of a transmission system for the proposed algorithm, where beamforming has been done by using the selected BP. Note that the beamforming by using the BP (i.e., beamformer) involves the use of a fixed set of weightings and time-delays, and it results in the formation of beams in an actual target direction at geographic coordinates, unlike adaptive beamforming techniques that consider the properties of the signals actually received by the array. Thus, beamforming by using the BP is much simpler to implement.

On the other hand, because the proposed algorithm changes the BP and TTP for the control channel part, its effects on the preamble and the traffic channel parts should be considered. There are a variety of scenarios in which this can be done. Firstly, the changed BP and TTP can be applied to only the control channel part without being applied to the preamble and traffic channel parts. Secondly, the changed BP and TTP applied to the control channel and preamble parts without being applied to the traffic channel part. These two cases increase only the receiving performance of the control channel, and operations related to the traffic channels are similar to those of conventional systems, with a slight difference in the channel state information (CSI) generation. Thirdly, we can apply the changed BP and TTP to all the parts. In this case, the change in the receiving environment caused by the changed BP and TTP can be considered as fluctuations induced by the short-term/long-term fading that depends on the algorithm period. Therefore, the entire operation will be the same as that in conventional systems. In this letter, the third scenario is assumed since it is more reasonable.

B. Example of Practical Implementation

Fig. 3 shows an example of the practical implementation of the proposed scheme, where we assume that one PBS and gr_{size} MBSs are controlled by the CBS. That is, $gr_{size} + 1$ BSs work together in the proposed algorithm. $BS0$ is the PBS and BSi

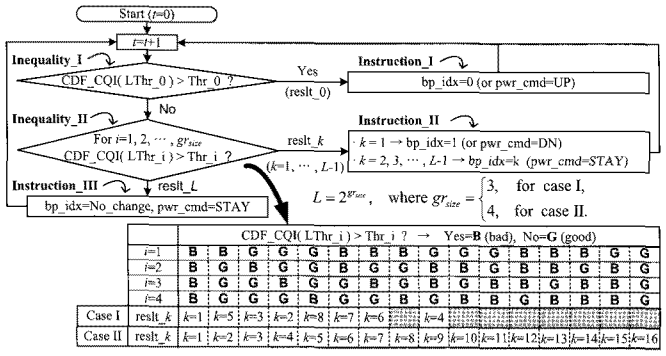

Fig. 3. Flowchart illustrating one example of practical implementation of the proposed algorithm for cases I and II.

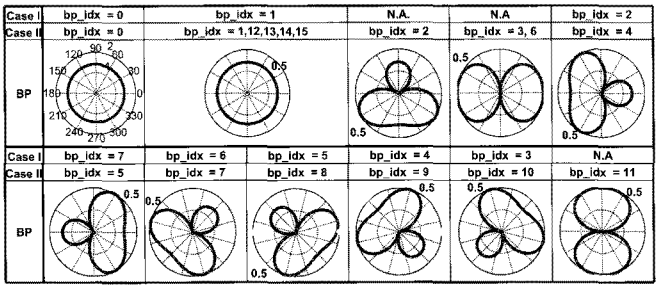

Fig. 4. Bps generated with $N = 2$ and $\Delta_t = 0.5$.

($i = 1, 2, \cdots, gr_{size}$) signifies the ith MBS. LThr_i and Thr_i are threshold values for BSi, and CDF_CQI($\cdot$) is the CDF function of the corresponding BS. These threshold values have been decided intuitively on the basis of the performances of the FCH channel and DL-MAP acquired by link-level simulation and the geometry/CQI distribution plotted from system-level simulation which does not employ the proposed algorithm. pwr_cmd is the command to control the TTP of the PBS, for example, UP, DN, and STAY. bp_idx is the index of the BP selected by the algorithm.

The flowchart can be summarized as follows: Initially ($t = 0$), the system parameters such as the initial TX power, MTP, up/down step size for power control, and initial BPs for the macro and pico cells are set to values that can be constant or updated periodically/non-periodically; t is the operation time. Next, each BS begins to transmit signals using the initial setting. Each MS sends a CQI to the PBS/MBS to which it belongs. Following this, each MBS or PBS sends the gathered CQI values to the CBS through the high-speed interface. The next time ($t = 1$), the CBS tests the veracity of several inequalities on the basis of information gathered from the PBS and the MBSs, and it then sends some instructions to one or multiple PBSs/MBSs, as shown in Fig. 3. Finally, the PBS or the MBSs perform some operations such as changing the BP and power control according to the given instructions. Note that the flowchart in Fig. 3 describes the operation of the PBS according to the proposed algorithm. In addition, the application of the proposed algorithm to several MBSs or PBSs is a straightforward process.

On the other hand, in Fig. 3, Inequality_I and Inequality_II are designed to test the interference environment of BSi. If CDF_CQI(3 dB) > 20 %, it indicates that the percentage of users with a CQI value lower than 3 dB is at least 20%. That is, if CDF_CQI(LThr_i) > Thr_i, it means that the receiving environment of the cell is poor and interference is relatively high. Instruction_I is used to improve the channel condition of PBS, and Instruction_II is used to enhance the channel conditions of MBSs when there is high interference. Instruction_III means that there is no operation.

IV. SIMULATION RESULTS

In this section, we discuss the performance of the proposed scheme obtained by system-level simulations when the algorithm of Fig. 3 and the BPs of Fig. 4 are used. The values of gr_{size} are 3 and 4 for cases I and II, respectively. In Fig. 4, bp_idx = 0 boosts power without beamforming. In contrast, bp_idx = 1 can be used to reduce power without beamforming. Note that the algorithm and the BPs are just one simple example of various possible implementations of the proposed scheme and have not been optimized for cases I and II.

Common channel beamforming is quite different from traffic channel beamforming. To improve the proportional fairness of the system (by giving different users more of a chance to be the best user) and to capture as much of the channel capacity as possible, conventional traffic channel beamforming needs some feedback strategies such as strategies for providing full/partial CSI or the corresponding index as feedback. In contrast, common channel beamforming rarely uses feedback information from MSs. Moreover, the common control channel is periodically transmitted with a predefined data rate. Thus, since there is no need to pursue a high received SINR beyond what is necessary, it is important to minimize the number of users with poor SINR values, i.e., outage users who cannot understand the common control channel information. In other words, reducing the number of outage users is more important than increasing the sum-rate capacity as far as the control channel is concerned.

On the basis of the above discussion, we employ the cumulative distribution function (CDF) of user geometry or the CQI (i.e., carrier-to-interference-and-noise ratio (CINR)) as a performance metric. In particular, we measure the increasing amount of low 20–30% on the CDF of users' geometry or CINR in order to investigate the outage probabilities for users on cell edges. If the curve of the CDF moves to the right, it means that there is an improvement in geometry, and thus, the number of outage users is reduced.

In every system-level simulation run, we consider the downlink of a 3-tier multi-cell wireless system with 19 macro cells and one pico cell, as shown in Fig. 1. The time delay between the CQI measurement and the change in BP is assumed to be 2 frames, which is a reasonable value for real systems. Details of the parameters are given in Table 1.

A. Case I

Basic simulation results obtained without the proposed algorithm are presented in Fig. 5, where [No PBS] and [Con] mean the typical wireless system with only 19 MBSs and the conventional HCS system with 19 MBSs and 1 PBS when the proposed algorithm is not used, respectively. We can see from this

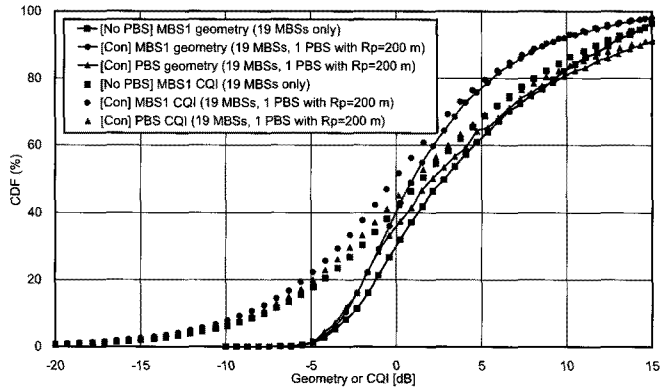

Fig. 5. CDFs of user geometry and CQI for case I when the proposed algorithm is not used. MTP of PBS is 20 dBm and $R_p = 200$ m.

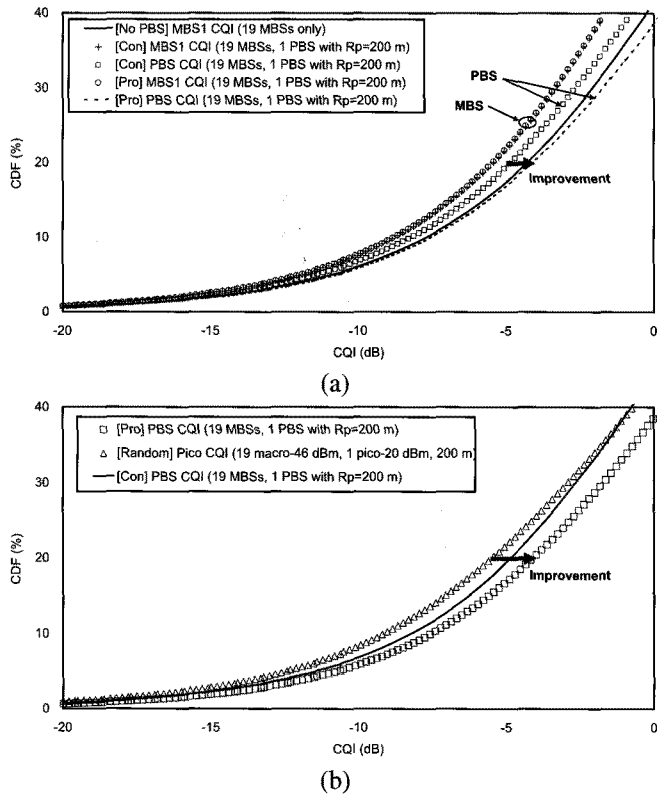

Fig. 6. The performance comparison in terms of CQI under case I when $R_p = 200$ m, MTP of PBS is 20 dBm, and the threshold values of SetA are used: (a) The proposed and conventional schemes and (b) the proposed and random BP schemes.

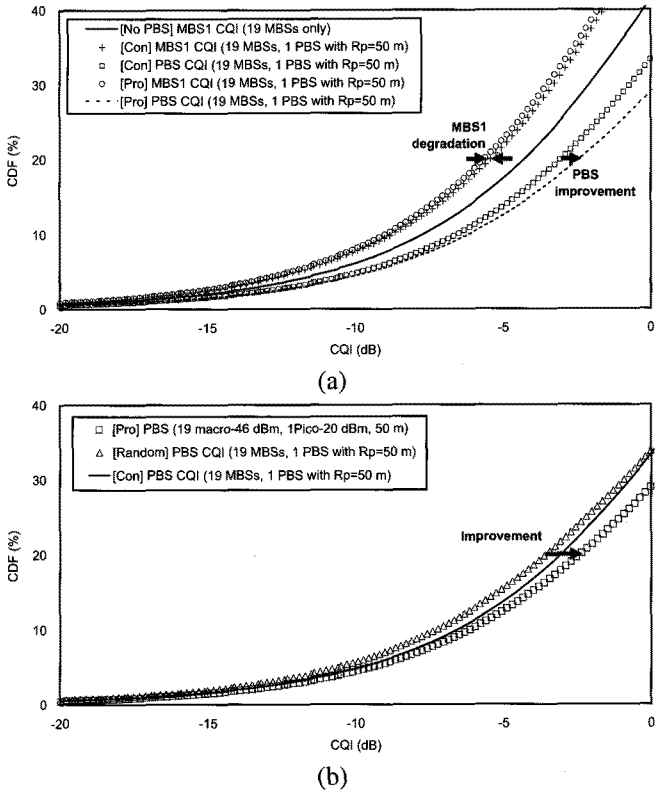

Fig. 7. The performance comparison in terms of CQI under case I when $R_p = 50$ m, MTP of PBS is 20 dBm, and the threshold values of SetB are used: (a) The proposed and conventional schemes and (b) the proposed and random BP schemes

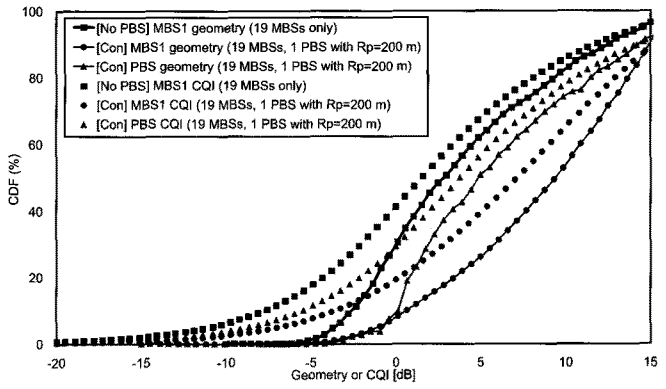

Fig. 8. CDFs of user geometry and CQI under case II when the proposed algorithm is not used. MTP of PBS is 20 dBm and $R_p = 200$ m.

figure that the distribution of the CQI is worse than that of geometry because of the effect of short-term fading. We can also observe that the CQI/geometry distribution of the MBS deteriorates considerably when PBSs are deployed within MBSs. This is because a PBS with a relatively large radius has been newly introduced into a region with very low interference levels, causing additional interference.

Fig. 6(a) shows the performance comparison between the proposed scheme and the conventional schemes when $R_p = 200$ m and the MTP of the PBS is 20 dBm. Here [Pro] signifies the HCS system with 19 MBSs and 1 PBS which employs the proposed algorithm. The threshold values in SetA were used in this simulation (see Table 2). From Fig. 6(a), we can see that the proposed scheme can improve the CQI distribution of the PBS without changing the CQI distribution of MBS1. The results for MBS2 and MBS3 were identical to that for MBS1, and therefore, we did not plot them.

In order to verify the effectiveness of the proposed scheme, we have tested the random BP scheme that randomly selects one of the given BPs without using the proposed algorithm. From Fig. 6(b), it is clear that the proposed scheme dominates the random BP scheme whose performance is denoted by [Random].

In order to investigate the effect of the cell radius, cases in

Table 2. Threshold values of the proposed algorithm used in simulations.

	SetA		SetB		SetC		SetD	
	LThr_i	Thr_i	LThr_i	Thr_i	LThr_i	Thr_i	LThr_i	Thr_i
PBS	−5 dB	20 %	−5 dB	13 %	−5 dB	11 %	0 dB	28 %
MBS1	−5 dB	20 %	−5 dB	20 %	−5 dB	7 %	0 dB	22 %
MBS2	−5 dB	20 %	−5 dB	20 %	−5 dB	17 %	0 dB	42 %
MBS3	−5 dB	18 %	−5 dB	20 %	−5 dB	17 %	0 dB	42 %
MBS4	-	-	-	-	−5 dB	18 %	0 dB	42 %

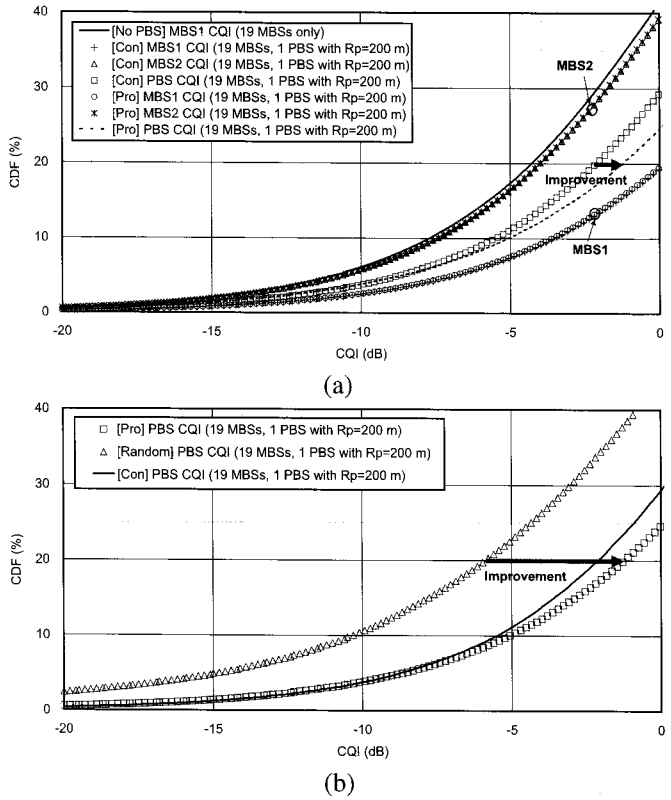

Fig. 9. The performance comparison in terms of CQI under case II when $R_p = 200$ m, MTP of PBS is 20 dBm, and the threshold values of SetC are used; (a) the proposed and conventional schemes and (b) the proposed and random BP schemes.

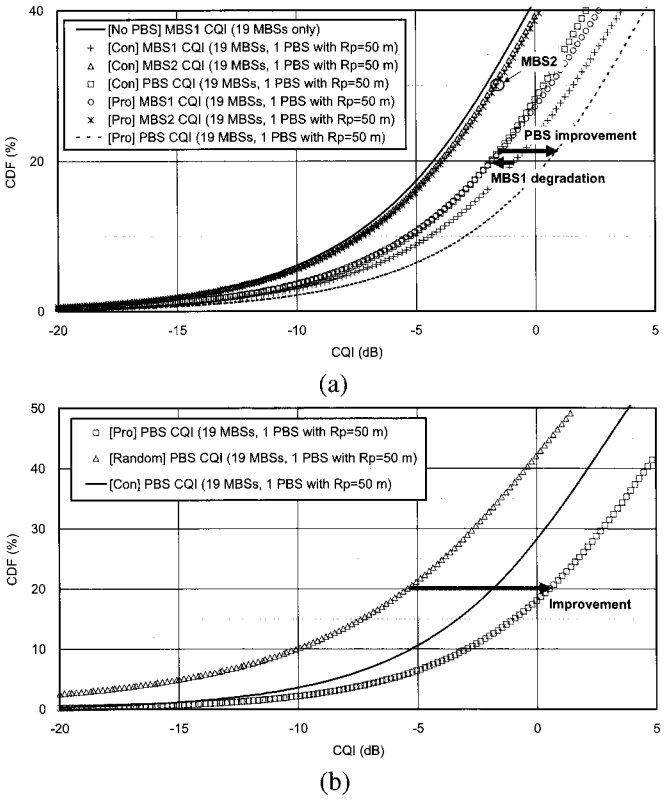

Fig. 10. The performance comparison in terms of CQI under case II when $R_p = 50$ m, MTP of PBS is 20 dBm, and the threshold values of SetD are used; (a) the proposed and conventional schemes and (b) the proposed and random BP schemes.

which the PBS had small cell radii were simulated. The cases showed trends similar to that for $R_p = 200$ m. The case where $R_p = 50$ m has been plotted in Fig. 7. From the figures, we can observe an overall performance improvement when the proposed scheme is utilized, even though the distribution of MBS1 slightly worsened. Note that the distributions of MBS2 and MBS3 remained unchanged and the threshold values of SetB were used for $R_p = 50$ m.

B. Case II

Fig. 8 shows basic simulation results obtained when the proposed algorithm was not used. We can also see that the distribution of CQI is worse than that of geometry. Unlike case I, the CQI/geometry distribution of MBS1 has improved considerably when PBSs are deployed within MBS1. This is because the PBS newly introduced into the region with a relatively high interference level has begun to support many of the users belonging to MBS1, who had suffered from interference.

Fig. 9(a) shows the performance comparison between the proposed scheme and the conventional schemes for $R_p = 200$ m when the MTP of the PBS is 20 dBm, and the threshold values of SetC are used. From Fig. 9(a), it is clear that the proposed scheme can improve the CQI distribution of the PBS without changing the CQI distributions of MBS1 and MBS2. MBS3 and MBS4 were largely unaffected by the proposed algorithm, and therefore, we did not plot them. As shown in Fig. 9 (b), the proposed scheme also outperformed the random BP scheme, as in case I.

We also simulated the cases in which the PBS has smaller cell radii for case II. The acquired results were similar to that for $R_p = 200$ m. However, some interesting results were obtained from the simulations. As shown in Fig. 10(a), we can improve the CQI distribution of PBS significantly if the degradation of the CQI distribution of MBS1 is allowed, where $R_p = 50$ m and the threshold values of SetD are used. Note that "[Pro] MBS1 CQI" is still better than "[No PBS] MBS1 CQI." Finally, we again observe that the proposed scheme dominates the random BP scheme, as shown in Fig. 10(b).

V. CONCLUSIONS

In this paper, we have presented a (semi-) centralized beamforming strategy for the performance enhancement of common control channel in HCS networks. In the proposed scheme,

beamforming is performed by using BP adaptively selected from predesigned BPs, and the total TX powers of the BSs is controlled together with the beamforming. These beamforming and power control cooperate closely in a complementary manner to mitigate interference that can be caused by beamforming and the increased TX power. This proposed scheme has been designed on the basis of an analysis of preliminary simulation results, which were acquired under optimistic and pessimistic interference scenarios from the viewpoint of the predesignated macro cell (i.e., cases I and II). In addition, we described a practical way for the implementation of the proposed scheme and presented some examples with low complexity for two-tier HCS networks consisting of macro and pico cells.

The performance of the proposed scheme was evaluated through multi-cell system-level simulations under the two scenarios. Simulation results confirmed that the proposed scheme is more advantageous than conventional systems in terms of reduction in the number of outage users, even though the algorithms and BPs used were not optimized for the two scenarios. Our next research step is to apply the proposed scheme to more generalized situations such as the coexistence of various types of cells. Finally, we believe that our investigations can be used as a guide for the further study of the performance enhancement of common control channels in HCS networks.

REFERENCES

[1] H. Claussen, "Performance of macro- and co-channel femtocells in a hierarchical cell structure," in *Proc. PIMRC*, Sept. 2007, pp. 1–5.

[2] V. Chandrasekhar, J.G. Andrews, and A. Gatherer, "Femtocell networks: A survey," *IEEE Commun. Mag.*, vol. 46, pp. 59–67, Sept. 2008.

[3] S. Kishore, L. J. Greenstein, H. V. Poor, and S. C. Schwartz, "Soft handoff and uplink capacity in a two-tier CDMA system," *IEEE Trans. Wireless Commun.*, vol. 4, no. 4, pp. 1297–1301, July 2005.

[4] Z. Shen and S. Kishore, "Optimal multiple access to data access points in tiered CDMA systems," in *Proc. IEEE VTC*, vol. 1, Sept. 2004, pp. 719–723.

[5] K. Huang, V. K. N. Lau, and Y. Chen, "Spectrum sharing between cellular and mobile ad hoc networks: transmission-capacity trade-off," *IEEE J. Sel. Areas Commun.*, vol. 27, no. 7, pp. 1256–1267, Sept. 2009.

[6] N. Jindal, J. G. Andrews, and S. Weber, "Bandwidth partitioning in decentralized wireless networks," *IEEE Trans. Wireless Commun.*, vol. 7, pp. 5408–5419, Dec. 2008.

[7] V. Chandrasekhar and J. G. Andrews, "Uplink capacity and interference avoidance for two-tier femtocell networks," *IEEE Trans. Wireless Commun.*, vol. 8, pp. 3498–3509, July 2009.

[8] NEC, "NEC's proposals for LTE Advanced," 3GPP RAN IMT Advanced Workshop, Shenzhen, China, REV-080022, Apr. 2008.

[9] "Air interface for fixed and mobile broadband wireless access systems," IEEE Std. 802.16e, 2006.

[10] Qualcomm Europe, "Evaluation methodology for LTE-A proposals," 3GPP TSG-RAN WG1 #53, Kansas City, Missouri, R1-081956, May 2008.

[11] Qualcomm Europe and Vodafone, "Evaluation methodology for LTE-A Heterogeneous networks," 3GPP TSG-RAN WG1 #53bis, Warsaw, Poland, R1-082554, June 30–July 4, 2008.

[12] Qualcomm Europe, "Categorization of technical proposals for the PHY layer of LTE-A," 3GPP TSG-RAN WG1 #53, Kansas City, Missouri, R1-081957, May 2008.

[13] Alcatel-Lucent, "Requirements and concepts for LTE Advanced," 3GPP RAN IMT Advanced Workshop, Shenzhen, China, REV-080044, Apr. 2008.

[14] "IEEE 802.16m evaluation methodology," IEEE 802.16 Broadband Wireless Access WG, IEEE 802.16m-08/004r1, Mar. 2008.

[15] "WINNER II Interim Channel Models," IST-WINNER II, IST-WINNER II Deliverable D1.1.1 v1.0, Dec. 2006.

[16] "Evaluation methodologies for the SLS with relay," 3GPP TSG RAN WG1 Meeting #54, Warsaw, Poland, R1-082396, June 30–July 4, 2008.

[17] ITU. (1997). Guidelines for the evaluation of radio transmission technologies for IMT-2000. [Online]. Available: http://www.itu.int

Cheolwoo You received the B.S., M.S., and Ph.D. degrees in Electronics Engineering from Yonsei University, Seoul, Korea, in 1993, 1995, and 1999, respectively. From January 1999 to April 2003, he worked as a Senior Research Engineer with the LG Electronics, Gyeonggi, Korea. During 2003–2004, he was a Senior Research Engineer at the EoNex, Songnam, Korea. From August 2004 to July 2006, he was with the Samsung Electronics, Suwon, Korea. He is currently an Associate Professor in the Dept. of Information and Communication Engineering, Myongji University, Korea. His research areas are next generation (4G) communication systems, air interface technologies in the international standards (PHY/MAC/cross layer), BS/MS modem design, communication theory, and signal processing. He is currently interested in advanced channel codes for mobile/nomadic communication systems, HARQ, new multiple access schemes, adaptive resource allocation, AMC, MIMO systems, cognitive radio, cooperative communication, home network, and relay schemes for 4G communication systems.

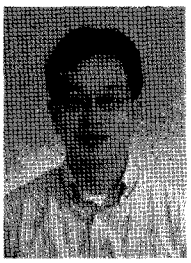

Young-Ho Jung received the B.S., M.S. and Ph.D. degrees in Electrical Engineering from Korea Advanced Institute of Science and Technology (KAIST), Daejeon, Korea, in 1998, 2000, and 2004, respectively. From 2004 to 2007, He had been with Samsung Advanced Institute of Technology (SAIT), and Samsung Electronics, Korea, and he was a Visiting Scholar in the Department of Electrical Engineering of Stanford University in 2005. Since 2007, he has been with the Department of Telecommunications Engineering, Korea Aerospace University, Goyang, Korea where he currently is an Assistant Professor. His primary research interests include cooperative communications, cross-layer optimization, air-interface design for IMT-Advanced systems, and mobile IPTV.

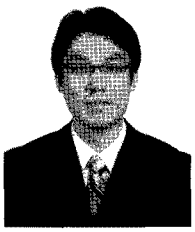

Sunghyun Cho received his B.S., M.S., and Ph.D. in Computer Science and Engineering from Hanyang University, Korea, in 1995, 1997, and 2001, respectively. From 2001 to 2006, he was with Samsung Advanced Institute of Technology, and with Telecommunication R&D Center of Samsung Electronics, where he has been engaged in the design and standardization of MAC and network layers of B3G, IEEE 802.16e, and WiBro/WiMAX systems. From 2006 to 2008, he was a Postdoctoral Visiting Scholar in the Department of Electrical Engineering, Stanford University. He is currently an Assistant Professor in the Department of Computer Science, Gyeongsang National University, Korea. His research interests include future wireless systems, vehicular communications, radio resource management, and cross layer design in wireless systems.